Electronic Supplementary Information (ESI)

for

High-valent iron (Fe^{VI}, Fe^{V}, and Fe^{IV}) species in water: Characterization and oxidative transformation of estrogenic hormones

Karolína Machalová Šišková,[1] Daniel Jančula,[2] Bohuslav Drahoš,[3] Libor Machala,[1] Pavel Babica,[2] Paula Godoy Alonso,[2] Zdeněk Trávníček,[3] Jiří Tuček,[1] Blahoslav Maršálek,[1,2] Virender K. Sharma,[4] Radek Zbořil[*,1]

[1] Regional Centre of Advanced Technologies and Materials, Departments of Physical Chemistry and Experimental Physics, Faculty of Science, Palacky University in Olomouc, Šlechtitelů 11, 783 71 Olomouc, Czech Republic.

[2] Institute of Botany, Academy of Sciences of the Czech Republic, Lidická 25/27, 602 00 Brno, Czech Republic.

[3] Regional Centre of Advanced Technologies and Materials, Department of Inorganic Chemistry, Faculty of Science, Palacky University in Olomouc, 17. listopadu 1192/12, 771 46 Olomouc, Czech Republic.

[4] Department of Environmental and Occupational Health, School of Public Health, Texas A&M University, 1266 TAMU, College Station, Texas 77843, U.S.A.

* Corresponding author: Phone: +420 585634337, Fax: +420 585634761, E-mail address: radek.zboril@upol.cz

Number of pages: 10

Number of figures: 9

Number of tables: 1

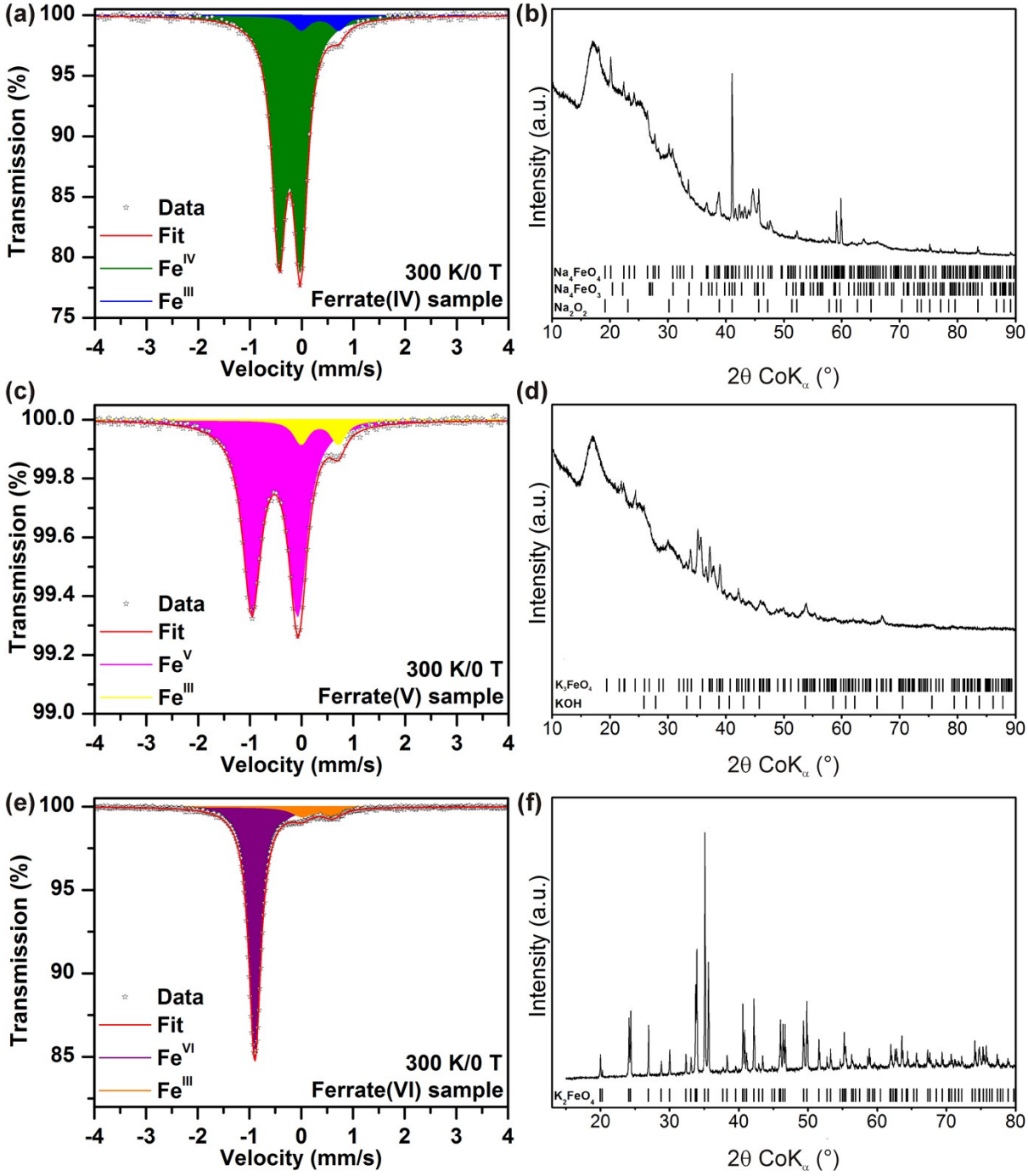

Fig. S1. ^{57}Fe Mössbauer spectra and X-ray diffraction pattern of initial ferrate(IV), ferrate(V), and ferrate(VI) samples used for degradation of estrogens: (a) Room-temperature ^{57}Fe Mössbauer spectrum and (b) X-ray powder diffraction pattern of ferrate(IV) compound (i.e., Na_4FeO_4). The values of hyperfine Mössbauer parameters, derived upon fitting the ^{57}Fe Mössbauer spectrum in panel (a), are listed in Table S1 with assignment of individual spectral components. The bars in panel (b) indicate the diffraction peaks of individual compounds found upon the analysis of the X-ray powder diffractogram. (c) Room-temperature ^{57}Fe Mössbauer spectrum and (d) X-ray powder diffraction pattern of ferrate(V) compound (i.e., K_3FeO_4). The values of hyperfine Mössbauer

parameters, derived upon fitting the ^{57}Fe Mössbauer spectrum in panel (c), are listed in Table S1 with assignment of individual spectral components. The bars in panel (d) indicate the diffraction peaks of individual compounds found upon the analysis of the X-ray powder diffractogram. (e) Room-temperature ^{57}Fe Mössbauer spectrum and (f) X-ray powder diffraction pattern of ferrate(VI) compound (i.e., K_2FeO_4). The values of hyperfine Mössbauer parameters, derived upon fitting the ^{57}Fe Mössbauer spectrum in panel (e), are listed in Table S1 with assignment of individual spectral components. The bars in panel (f) indicate the diffraction peaks of individual compounds found upon the analysis of the X-ray powder diffractogram.

Table S1. Values of the Mössbauer hyperfine parameters, derived from the fitting of the room-temperature ^{57}Fe Mössbauer spectrum of ferrate(IV), ferrate(V), and ferrate(VI), where δ is the isomer shift, ΔE_Q is the quadrupole splitting, and RA is the relative spectral area of individual spectral components identified during spectrum fitting.

Sample	Component	$\delta \pm 0.01$ (mm/s)	$\Delta E_Q \pm 0.01$ (mm/s)	RA ± 1 (%)	Assignment
Ferrate(IV)	Doublet	– 0.23	0.41	94	Fe^{IV}
	Doublet	0.35	0.73	6	Fe^{III}
Ferrate(V)	Doublet	– 0.51	0.89	93	Fe^{V}
	Doublet	0.35	0.72	7	Fe^{III}
Ferrate(VI)	Singlet	– 0.90	------	96	Fe^{VI}
	Doublet	0.34	0.72	4	Fe^{III}

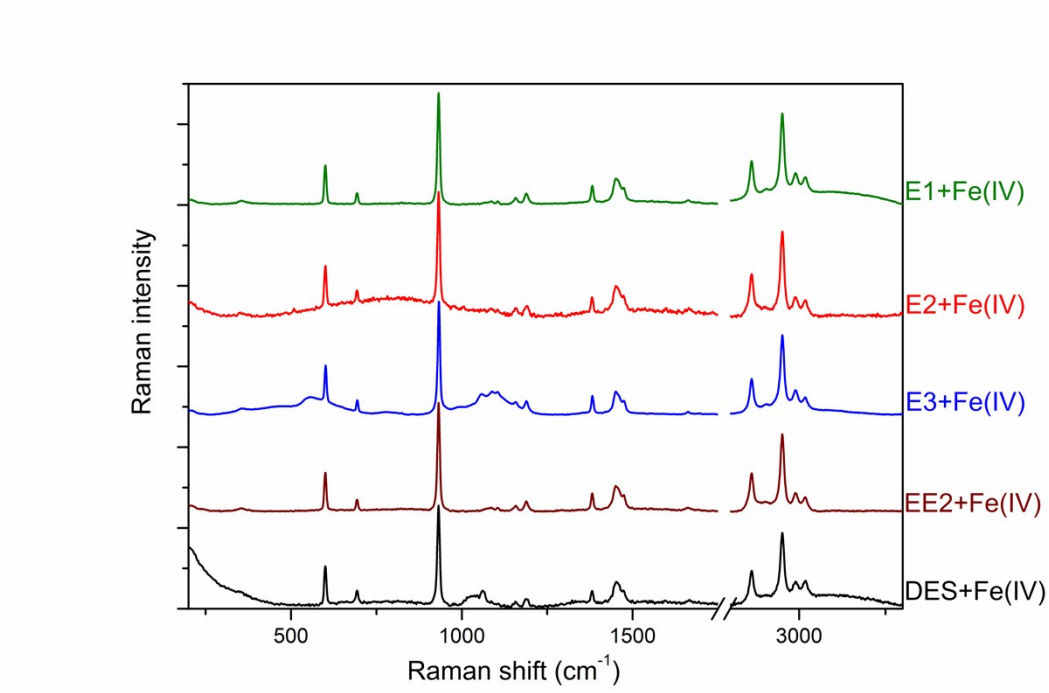

Fig. S2. Comparison of the Raman spectra of degradation products of E1, E2, E3, EE2, and DES estrogens after the treatment with ferrate(IV). The spectra are normalized with respect to the most intensive peak (located at 934 cm^{-1}).

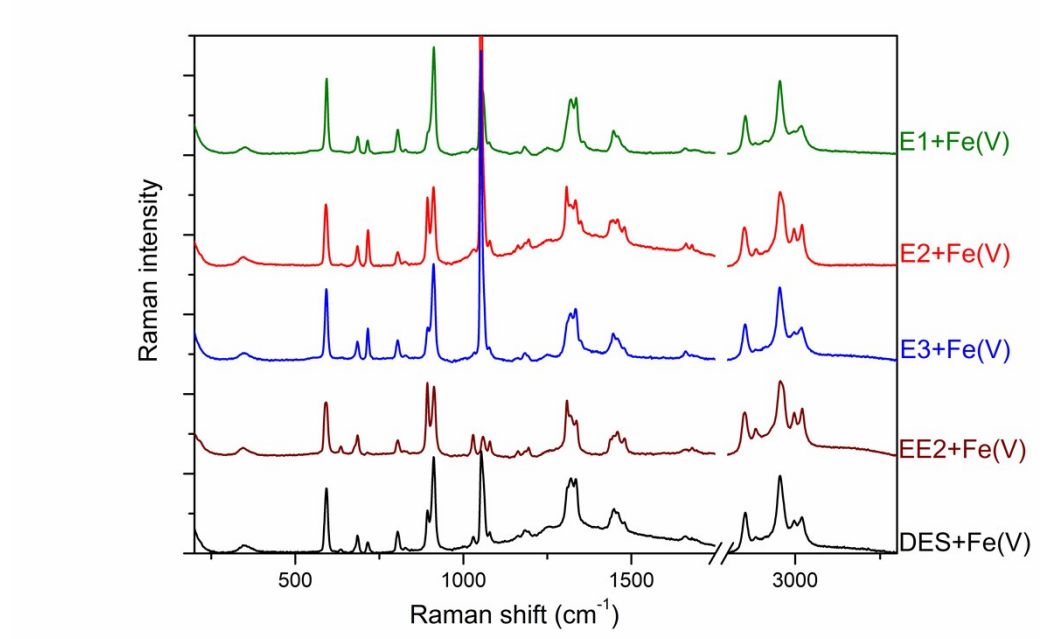

Fig. S3. Comparison of the Raman spectra of degradation products of E1, E2, E3, EE2, and DES estrogens after treatment with ferrate(V). The spectra are normalized with respect to the peak located at 2953 cm^{-1} for the sake of the visualization of less intensive peaks.

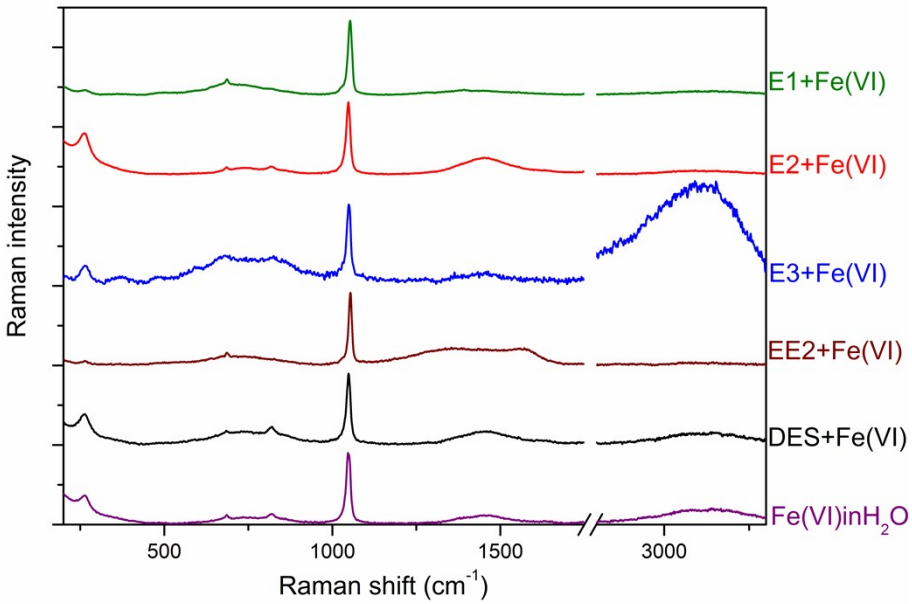

Fig. S4. Comparison of the Raman spectra of degradation products of E1, E2, E3, EE2, and DES estrogens after treatment with ferrate(VI). Raman spectrum of K_2FeO_4 dissolved in water is shown for the sake of a direct comparison. The spectra are normalized with respect to the most intensive peak (located at 1048 cm^{-1}).

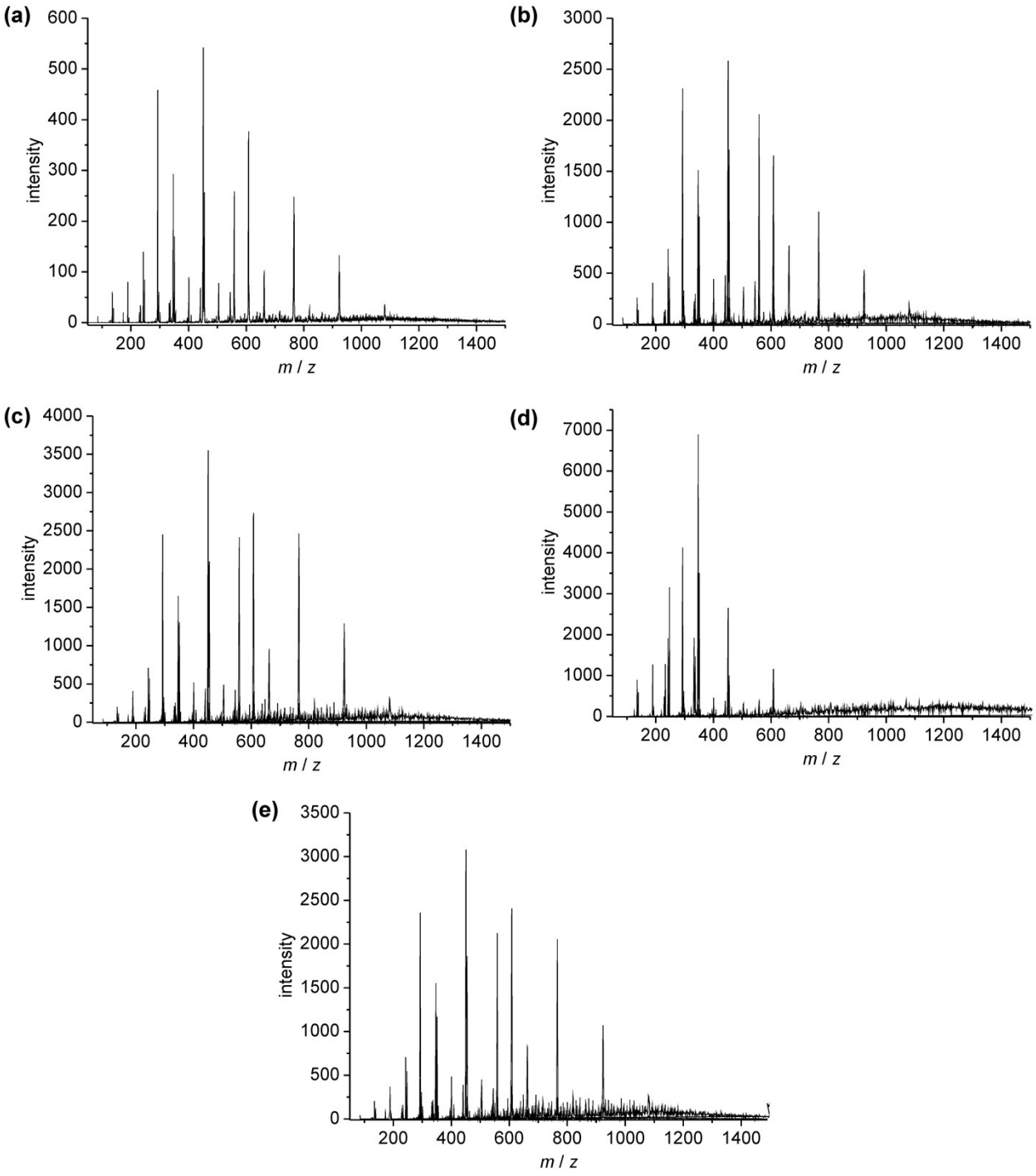

Fig. S5. Comparison of full ESI mass spectra of degradation products of (a) E1, (b) E2, (c) E3, (d) EE2, and (e) DES estrogens after treatment with ferrate(IV).

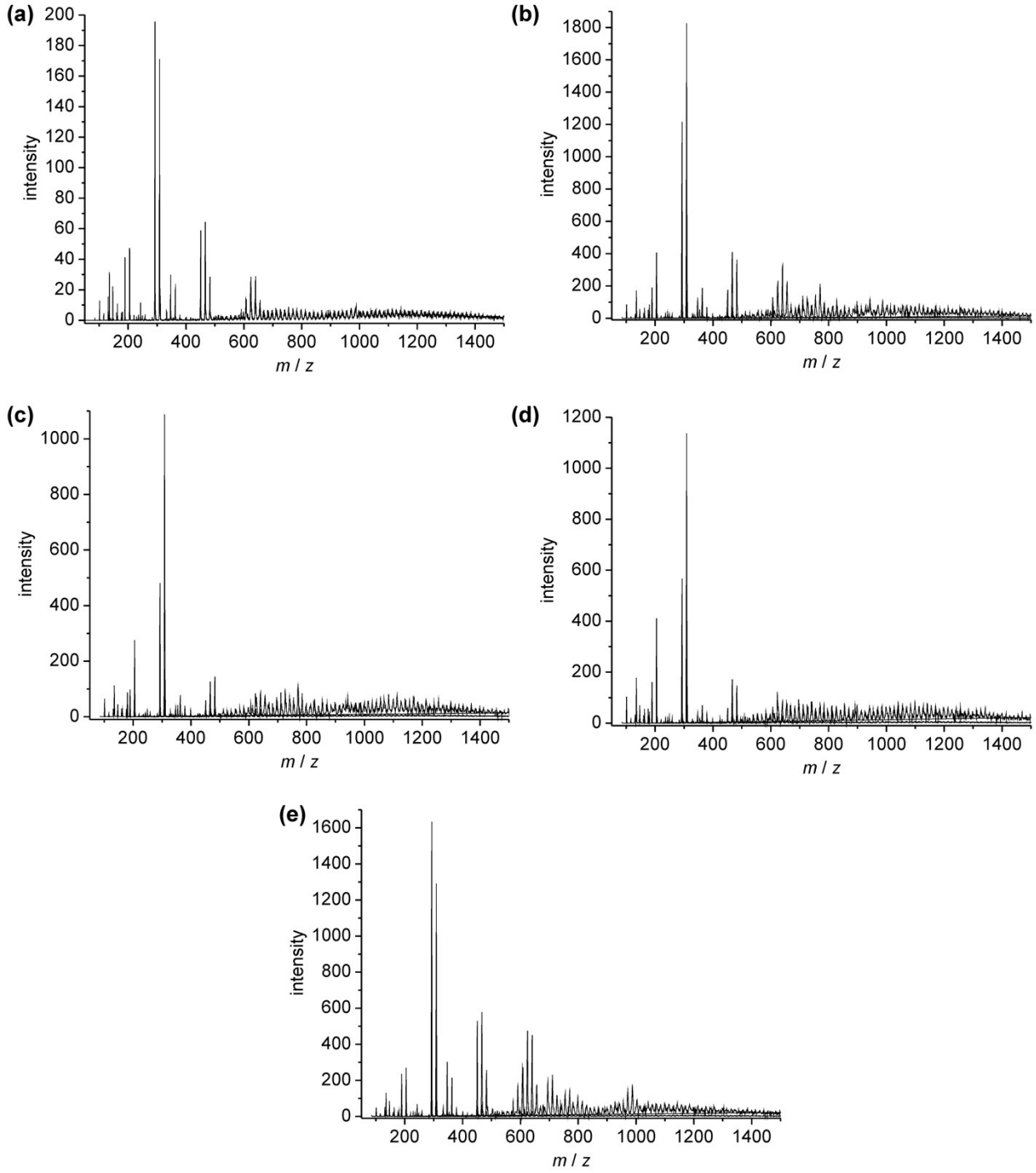

Fig. S6. Comparison of full ESI mass spectra of degradation products of (a) E1, (b) E2, (c) E3, (d) EE2, and (e) DES estrogens after treatment with ferrate(V).

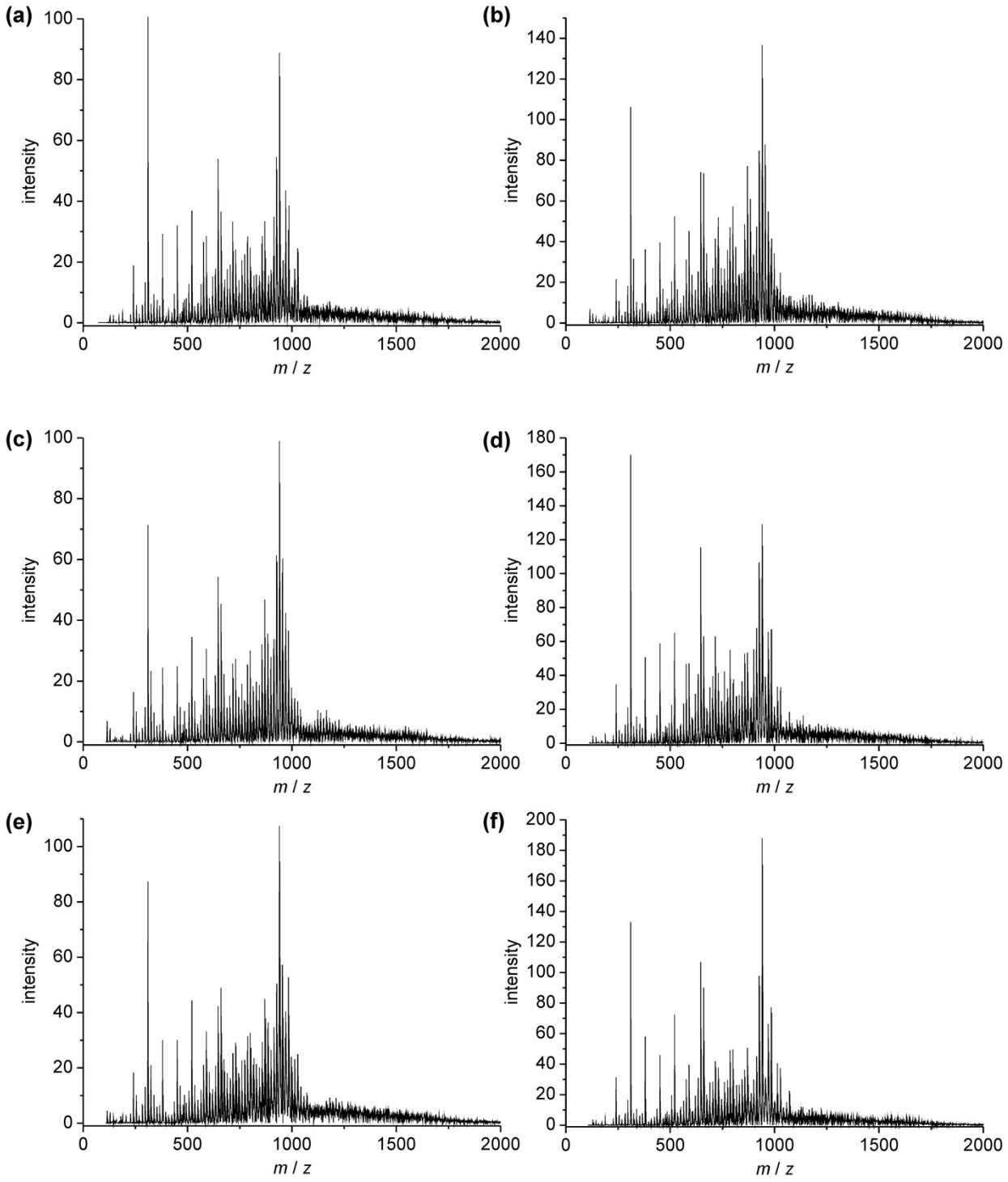

Fig. S7. Comparison of full ESI mass spectra of degradation products of (a) E1, (b) E2, (c) E3, (d) EE2, and (e) DES estrogens after treatment with ferrate(VI) together with (f) ESI mass spectrum of pure K_2FeO_4 decomposed in water/MeOH.

Product ID	APCI(+)-MS *m/z*	Proposed structure	R_t / min
E1	271	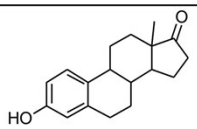	27.5
1	285	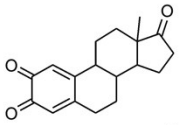	21.8
2	287	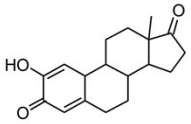	18.7
3	301	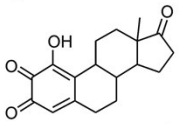	15.7
4	321	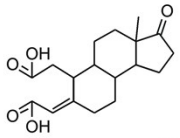	23.5
5	323	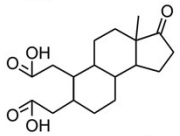	23.5
6	239	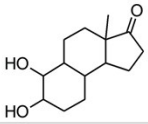	11.1

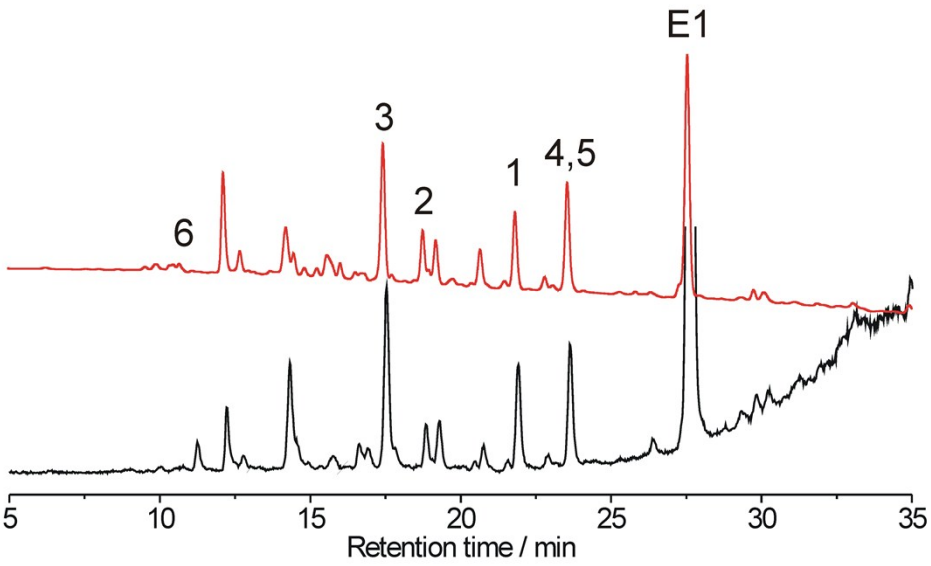

Fig. S8. Data from HPLC-MS analysis of E1 degradation by ferrate(VI) (UV-VIS detector (230 nm) – in red color, positive MS mode (total ion current) in black color) together with the table summarizing the proposed structures of the observed intermediates with the corresponding masses, retention times, and assignment (positions) in chromatogram. The intermediates are numbered according to the oxidation pathway.

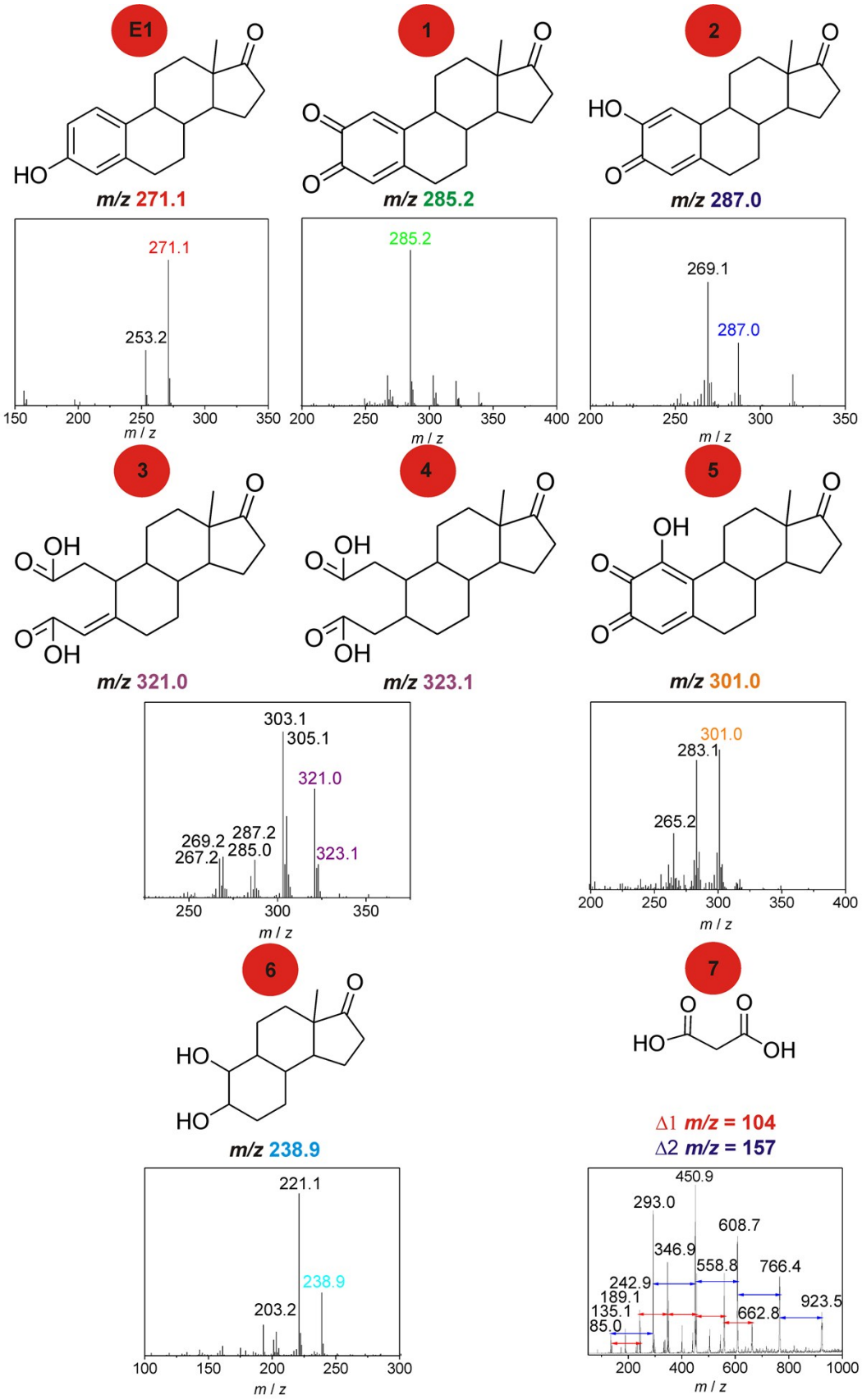

Fig. S9. Structural formulas and ESI mass spectra of intermediates of E1 degradation by ferrate(VI).